



SHORT COMMUNICATION

A High Serum Iron Level Causes Mouse Retinal Iron Accumulation Despite an Intact Blood-Retinal Barrier

Liangliang Zhao,^{*†} Yafeng Li,[†] Delu Song,[†] Ying Song,[†] Milan Theurl,[†] Chenguang Wang,^{*†} Alyssa Cwanger,[†] Guanfang Su,^{*} and Joshua L. Dunaief[†]

From the Department of Ophthalmology,* The Second Hospital of Jilin University, Jilin, China; and the F.M. Kirby Center for Molecular Ophthalmology,[†] Scheie Eye Institute, University of Pennsylvania, Philadelphia, Pennsylvania

Accepted for publication
July 17, 2014.

Address correspondence to
Joshua L. Dunaief, M.D.,
Ph.D., 305 Stellar Chance Labs,
422 Curie Blvd., Philadelphia,
PA 19104. E-mail: jdunaief@upenn.edu

The retina can be shielded by the blood-retinal barrier. Because photoreceptors are damaged by excess iron, it is important to understand whether the blood-retinal barrier protects against high serum iron levels. Bone morphogenetic protein 6 (Bmp6) knockout mice have serum iron overload. Herein, we tested whether the previously documented retinal iron accumulation in Bmp6 knockout mice might result from the high serum iron levels or, alternatively, low levels of retinal hepcidin, an iron regulatory hormone whose transcription can be up-regulated by Bmp6. Furthermore, to determine whether increases in serum iron can elevate retinal iron levels, we i.v. injected iron into wild-type mice. Retinas were analyzed by real-time quantitative PCR and immunofluorescence to assess the levels of iron-regulated genes/proteins and oxidative stress. Retinal hepcidin mRNA levels in Bmp6 knockout retinas were the same as, or greater than, those in age-matched wild-type retinas, indicating that Bmp6 knockout does not cause retinal hepcidin deficiency. Changes in mRNA levels of L ferritin and transferrin receptor indicated increased retinal iron levels in i.v. iron-injected wild-type mice. Oxidative stress markers were elevated in photoreceptors of mice receiving i.v. iron. These findings suggest that elevated serum iron levels can overwhelm local retinal iron regulatory mechanisms. (*Am J Pathol* 2014, 184: 2862–2867; <http://dx.doi.org/10.1016/j.ajpath.2014.07.008>)

Iron is necessary for life, but in excess it can be toxic. Therefore, iron is tightly regulated. Many of the genes that regulate iron on the systemic level are expressed in the retina and may play a role in local iron regulation.¹ We previously studied double knockout (KO) mice deficient for the iron-exporting ferroxidases ceruloplasmin and hephaestin.² These double KO mice have age-dependent retinal iron accumulation and degeneration.^{3,4} Double KO mice have retinal iron overload despite systemic iron deficiency, so it is likely that the retina accumulates iron as a result of impaired retinal iron export. We also studied mice with systemic knockout of the iron-regulatory hormone hepcidin (*Hamp*). These mice also have age-dependent retinal iron accumulation with degeneration.⁵ Bone morphogenetic protein 6 (Bmp6) is known to up-regulate *Hamp* in the liver and retina,⁶ and *Bmp6* KO mice have retinal iron accumulation similar to *Hamp* KO mice.⁷ Because *Hamp* and *Bmp6* KO mice have elevated serum iron levels, it is unclear whether the retinal iron accumulation in these mice results from elevated serum iron levels caused by

diminished liver *Hamp* production or from low retinal *Hamp* levels impairing local iron regulation in the retina.

There are several routes for iron influx yet only one for cellular iron efflux^{8–10}; the transmembrane protein ferroportin can export iron out of cells. Ferroportin can be regulated by the 25 amino acid hepcidin peptide, which triggers its internalization and degradation, leading to decreased export of cellular iron.¹¹ *Hamp* expression in the liver is increased by iron overload, and, after secretion into the bloodstream, limits intestinal iron absorption, macrophage iron recycling, and hepatocyte iron release. In comparison, iron deficiency anemia and tissue hypoxia can inhibit *Hamp* expression to increase the iron supply for the body.^{12–14}

Supported by NIH grant EY015240, Research to Prevent Blindness, the F.M. Kirby Foundation, the Paul and Evanina Bell Mackall Foundation Trust (all to J.L.D.), and a gift in memory of Dr. Lee F. Mauer.

L.Z. and Y.L. contributed equally to this work.

Disclosures: None declared.

Hamp is expressed in many tissues, including the retina within photoreceptors, Müller cells, and retinal pigment epithelium (RPE).¹⁵ Ferroportin, the target of hepcidin, is localized to RPE, the photoreceptor inner segment, the outer plexiform layer, and the inner limiting membrane.¹⁶ Locally synthesized *Hamp* may regulate ferroportin in the neural retina (NR). To determine whether retinal hepcidin deficiency contributes to the retinal iron accumulation in *Bmp6* KO mice, we compared *Hamp* mRNA levels in *Bmp6* KO versus wild-type (WT) mice. We also tested whether WT mice given i.v. injections of iron sucrose would develop retinal iron accumulation despite the presence of *Hamp* synthesized locally in the retina.

Materials and Methods

Animals

Bmp6 KO mice on the CD1 background were generated as described previously.¹⁷ *Bmp6* KO male mice aged 2.5, 3.5, 5, and 10 months and age-matched WT male CD1 mice were used for the experiments. WT C57BL/6J mice at 2.5 months were obtained from The Jackson Laboratory (Bar Harbor, ME). C57BL/6J mice were treated with or without 1.2 mg of iron sucrose (Venofer; American Regent, Shirley, NY) in 200 mL of 0.9% saline solution via tail vein injection three times (once per week) until sacrifice.

Experimental procedures were performed in accordance with the Association for Research in Vision and Ophthalmology statement for the use of animals in ophthalmology and vision research. All the protocols were approved by the Institutional Animal Care and Use Committee of the University of Pennsylvania (Philadelphia, PA). The eyes were enucleated immediately after death and were fixed overnight in 4% paraformaldehyde for immunofluorescence.

Immunolabeling

Mouse globes fixed in 4% paraformaldehyde were rinsed in phosphate-buffered saline, and the eyecups were dissected. The eyecups were cryoprotected in 30% sucrose solution overnight and then embedded in optimal cutting temperature compound (Tissue-Tek; Sakura Finetek USA Inc., Torrance, CA) and slowly frozen in 2-methylbutane on dry ice. Immunofluorescence was performed on sections 10 μ m thick, as described previously.¹⁸ Primary antibodies were rabbit anti-L ferritin (E17) at 1:200 dilution [a gift from Dr. Paolo Arosio (University of Brescia, Brescia, Italy)], rabbit anti-malondialdehyde (MDA) at 1:100 dilution (Alpha Diagnostic, San Antonio, TX), and rabbit anti-4-hydroxy-nonenal (HNE) at 1:100 dilution (Alpha Diagnostic). Primary antibody was detected using fluorophore-labeled secondary antibody (Jackson ImmunoResearch Laboratories, West Grove, PA). Control sections were treated identically except that primary antibodies were omitted. Sections were analyzed by

fluorescence microscopy with identical exposure parameters using a Nikon TE300 microscope equipped with ImagePro Plus software version 6.1 (Media Cybernetics Inc., Bethesda, MD).

RPE Isolation

We used a recently developed method for the rapid isolation of RPE cells for RNA extraction and analysis.¹⁹ This method uses simultaneous RPE cell isolation and RNA stabilization. Briefly, eyes were enucleated and placed on an ice-cold phosphate-buffered saline-soaked sponge. The periocular tissues were removed, the eye was opened posterior to the limbus using Vannas scissors, and the anterior segment and the retina were removed. The resulting posterior eyecups were quickly dipped into a phosphate-buffered saline-containing microcentrifuge tube to remove any loosely adherent debris. Afterward, the eyecup was immediately transferred to a microcentrifuge tube containing 200 μ L of ice-cold RNeasy lysis reagent (Cat. No. 76526; Qiagen Inc., Valencia, CA), with gentle manual tapping of the tube every 1 to 2 minutes to accelerate the release of RPE cells. After 10 minutes, the eyecup was removed from the solution using forceps. RPE cells were then centrifuged (5 minutes at 2750 rpm). The RNA isolation was performed using an RNeasy plus micro kit (Cat. No. 74034; Qiagen Inc.) according to the manufacturer's protocol.

Real-Time Quantitative PCR

Liver, NR, and RPE samples obtained from *Bmp6* KO and WT mice were analyzed using real-time quantitative PCR for gene expression, as described previously.²⁰ RNA isolation was performed using an RNeasy mini kit (Cat. No. 74106; Qiagen Inc.) according to the manufacturer's protocol. The RNA was quantified using a spectrophotometer and was stored at -80°C . cDNA was synthesized using TaqMan reverse transcription reagents (Cat. No. 808-0234; Applied Biosystems, Foster City, CA) according to the manufacturer's protocol. TaqMan gene expression assays were obtained from Applied Biosystems and were used for PCR analysis. Probes included hepcidin antimicrobial peptide (Mm04231240_s1), transferrin receptor (Tfrc, Mm00441941_m1), L ferritin (Mm03030144_g1), von Willebrand factor homolog (Mm00550376_m1), retinal pigment epithelium 65 (Rpe65, Mm00504133_m1), and collagen, type VI, alpha 1 (Mm00487160_m1). Eukaryotic 18S rRNA (Hs99999901_s1) served as an internal control owing to its constant expression level among the studied sample sets. Real-time TaqMan RT-PCR (Applied Biosystems) was performed using an ABI Prism 7500 detection system and the $\Delta\Delta\text{C}_T$ method, which provided normalized expression values. The amount of target mRNA was compared among groups of interest. All reactions were performed in biological (three mice) and technical (three real-time PCR replicates per mouse) triplicates.

Statistical Analysis

The means \pm SEM were calculated for each comparison group. Statistical analysis was performed using Student's two-group, two-sided *t*-test. For multiple comparisons, we used one-way analysis of variance with post hoc pairwise comparisons using Bonferroni correction for multiple comparisons. $P < 0.05$ was considered statistically significant. All statistical analyses were performed using GraphPad Prism software version 5 (GraphPad Software Inc., San Diego, CA).

Results

Regulation of Hamp in NR in Response to Iron Status

Expression of *Hamp* in the liver, a key regulator of systemic iron metabolism, can be up-regulated by Bmp6.³ Consistent with a previous report,⁶ Hamp mRNA levels in the livers of male *Bmp6* KO mice at several ages were diminished compared with those in WT male mice (Figure 1, A–C).

Because the Bmp6 pathway can increase Hamp expression at the systemic level, to determine whether it can also regulate

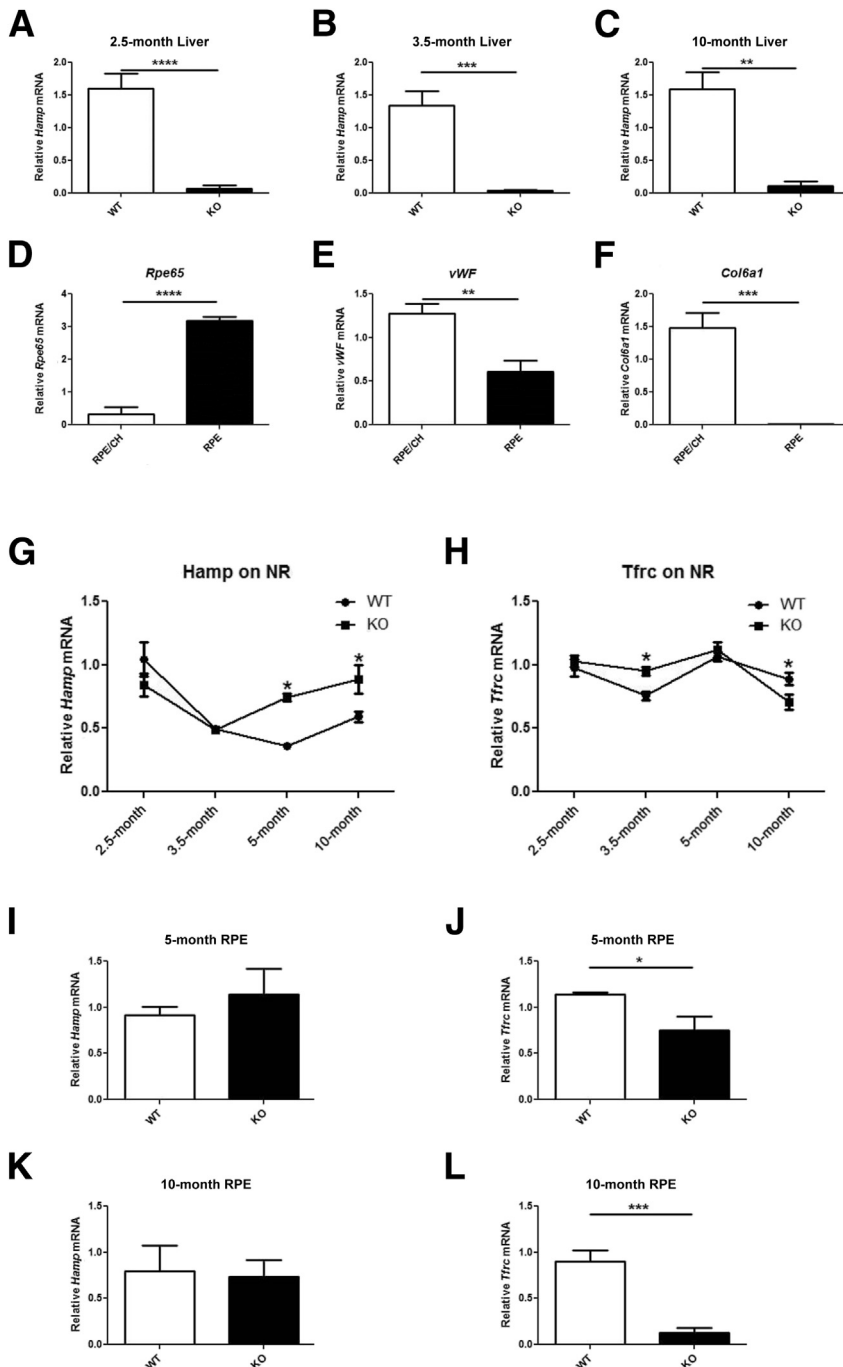


Figure 1 Quantitative PCR results in liver, NR, RPE/choroid (CH), and isolated RPE of *Bmp6* KO and WT mice. *Bmp6* KO mice had lower Hamp mRNA levels in liver than did age- and sex-matched WT controls at 2.5 months (A), 3.5 months (B), and 10 months (C) of age. Relative mRNA levels of RPE65 (D), von Willebrand factor homolog (vWF) (E), and collagen VI (Col6a1) (F) in RPE/CH versus isolated RPE. RPE samples had enriched RPE65, limited vWF, and barely detectable Col6a1 mRNA levels compared with RPE/CH. Relative mRNA levels of Hamp (G, I, and K) and Tfrc (H, J, and L) in NR of *Bmp6* KO and WT mice at different ages. G: Hamp mRNA levels in 2.5- and 3.5-month-old *Bmp6* KO mice were not different from those in WT controls. However, Hamp mRNA levels were significantly higher in 5- and 10-month-old *Bmp6* KO mice compared with WT controls. H: Tfrc mRNA levels in *Bmp6* KO NR showed no significant difference at 2.5 and 5 months and was decreased at 3.5 and 10 months compared with age- and sex-matched WT mice. I and K: Hamp mRNA levels in RPE showed no significant difference between *Bmp6* KO mice and WT mice at 5 and 10 months. J and L: However, Tfrc mRNA levels showed a significant decrease in *Bmp6* KO mice compared with WT controls at 5 and 10 months. Values shown are means \pm SEM of $\Delta\Delta C_T$. $N = 3$ biological and technical replicates for all real-time quantitative PCR experiments. * $P < 0.05$, ** $P < 0.01$, *** $P < 0.001$, and **** $P < 0.0001$.

retinal Hamp we measured Hamp mRNA levels in NR and RPE. First, to test the level of RPE RNA enrichment in isolated RPE cells, we measured mRNA levels of RPE65, an RPE-specific marker, which was almost sixfold higher in purified RPE samples compared with the RPE/choroid samples. In addition, the von Willebrand factor homolog and collagen VI mRNA levels, which are expressed in choroid and sclera, were decreased significantly in purified RPE samples compared with RPE/choroid samples (Figure 1, D–F).

Hamp mRNA levels in NR showed no significant difference between *Bmp6* KO and WT mice at 2.5 and 3.5 months and increased in *Bmp6* KO compared with WT mice aged 5 to 10 months (Figure 1G). *Tfrc* mRNA levels in *Bmp6* KO NR showed no significant difference at 2.5 months, were decreased at 3.5 months, were unchanged at 5 months, and were decreased at 10 months (Figure 1H) in *Bmp6* KO mice compared with age- and sex-matched WT mice. Decreased *Tfrc* mRNA levels indicate elevated iron levels because increased intracellular iron prevents IRP1 and IRP2 from stabilizing *Tfrc* mRNA.²¹

Hamp mRNA levels in RPE showed no significant differences between *Bmp6* KO mice and WT mice at 5 and 10 months (Figure 1, I and K, respectively). *Tfrc* mRNA levels in RPE showed a significant decrease in *Bmp6* KO mice compared with WT mice (Figure 1, J and L).

Eyes from C57BL/6J Mice Treated with I.V. Iron Have Increased L Ferritin and Oxidative Stress Markers

The levels of the cytosolic iron storage protein ferritin are regulated by labile iron levels through iron regulatory proteins IRP1 and IRP2.²¹ Accordingly, when labile iron levels rise, ferritin translation increases, leading to increasing levels of L ferritin and H ferritin proteins.²² RPE cells showed L ferritin immunoreactivity that was stronger in mice treated with i.v. iron than in age-matched controls (Figure 2, A–D). Iron accumulation–induced lipid peroxidation was assessed by immunofluorescence detection of MDA and HNE. These are reactive intermediates in the formation of advanced lipid peroxidation end products. Thus, they are frequently measured as indicators of lipid peroxidation and oxidative stress. We detected an increase of MDA and HNE in the inner segment and outer plexiform layers of mice that were injected with iron compared with controls (Figure 2, E–H).

Hamp, L Ferritin, and Transferrin Receptor mRNA Levels in C57BL/6J Mice Treated with I.V. Iron

In C57BL/6J mice treated with three weekly i.v. iron sucrose injections, Hamp and L ferritin mRNA levels were significantly higher in the liver compared with control mice

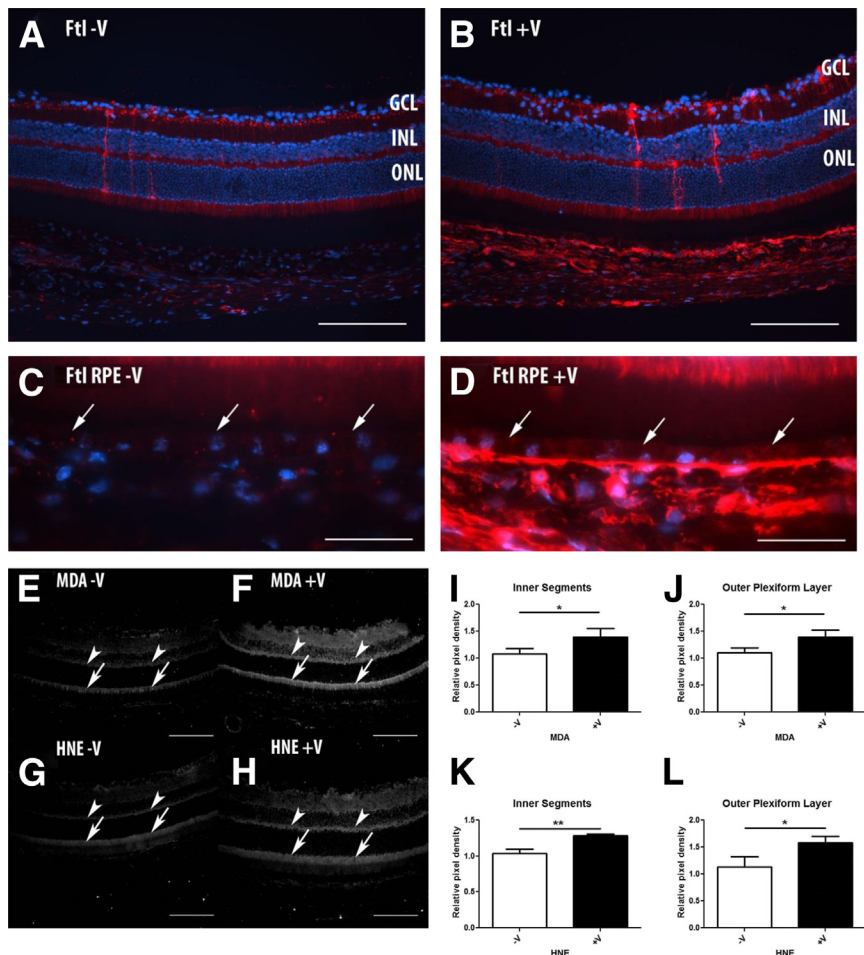


Figure 2 Iron labeling in RPE of i.v. iron sucrose–injected C57BL/6J mice. Iron level as determined by immunolabeling for L ferritin (Ftl; red) was greater in the RPE of iron sucrose (V)–injected mice (B) compared with controls (A). C and D show the high magnification (60× objective) of the RPE layer (arrows) in A and B, respectively. Oxidative stress levels determined by immunolabeling for MDA and HNE were greater in inner segments (arrows) and outer plexiform layers (arrowheads) with iron sucrose injection (F and H) compared with controls (E and G). I–L: Pixel density quantification of MDA and HNE immunostaining in the inner segments and outer plexiform layer of three mice with iron sucrose injection or controls. Statistical analysis was performed using Student’s two-group, two-sided *t*-test. **P* < 0.05, ***P* < 0.01. Scale bars: 100 μm (A, B, E–H); 33.3 μm (C and D). GCL, ganglion cell layer; INL, inner nuclear layer; ONL, outer nuclear layer.

(Figure 3, A and C), whereas *Tfrc* mRNA levels were unchanged (Figure 3B). *Hamp* mRNA levels were not significantly different in NR and RPE of mice treated with or without iron (Figure 3, D and G). *Tfrc* mRNA levels were significantly lower in NR of iron-treated mice compared with control mice (Figure 3E), whereas L ferritin mRNA levels (a less sensitive measure of iron) were unchanged (Figure 3F). L ferritin mRNA levels were significantly higher in the RPE of iron sucrose–injected mice compared with controls, and *Tfrc* mRNA levels were significantly lower (Figure 3, H and I).

Discussion

Previous studies showed elevated serum and retinal iron levels in systemic *Hamp* and *Bmp6* KO mice.^{5,7} To determine whether the retinal iron accumulation was due to loss of *Bmp6*-stimulated retinal production of *Hamp*, we measured *Hamp* mRNA in NR and RPE by real-time quantitative PCR in *Bmp6* KO mice. These results indicate an important influence of systemic *Hamp* (and, consequently, serum iron) levels on retinal iron. In *Bmp6* KO mice, liver but not retinal *Hamp* levels were diminished.

Bmp6 can up-regulate *Hamp* expression systemically, and we hypothesized that there was a similar local regulatory mechanism in the retina. Despite retinal expression of *Bmp6* and its receptors, retinal *Hamp* expression was not diminished in *Bmp6* KO mice; it increased significantly. These results provide evidence that basal retinal *Hamp* expression is independent of the *Bmp6* pathway. As the retina takes in more iron from the iron-rich blood in *Bmp6*

KO mice, this iron seems to up-regulate *Hamp* expression. As a measure of retinal iron levels, *Tfrc* mRNA levels at 2.5 months were similar between KO and WT mice. *Tfrc* levels were decreased at age 3.5 months, indicating elevated retinal iron levels. At 5 months, *Hamp* expression in NR was increased in *Bmp6* KO mice, possibly diminishing the iron influx, as *Tfrc* levels were normal. However, at 10 months, *Hamp* levels were still higher in *Bmp6* KO mice than in age-matched WT mice, but *Tfrc* levels were lower in KO mice, suggesting that the increased *Hamp* levels were insufficient to prevent further iron influx.

In RPE, 5- and 10-month-old *Bmp6* KO mice had decreased *Tfrc* mRNA levels compared with age- and sex-matched WT mice. This reflects increased RPE iron levels caused by high systemic iron levels; a reduction in local retinal *Hamp* levels was not responsible because there was no difference in RPE *Hamp* mRNA levels between *Bmp6* KO mice and WT mice.

To further assess the effects of elevated systemic iron levels on retinal iron, we injected mice with i.v. iron sucrose, which is used in patients to treat iron deficiency anemia. After three weekly i.v. injections, we confirmed that liver *Hamp* mRNA levels increased, reflecting elevated hepatocyte iron levels. *Tfrc* levels did not change in the liver, suggesting that subpopulations of liver cells did not experience enough of an iron load to down-regulate *Tfrc* mRNA. In the RPE and NR of iron sucrose–treated mice, *Tfrc* mRNA levels decreased compared with controls. L ferritin mRNA levels increased in the RPE of iron sucrose–injected mice. These results show that in WT mice, high systemic iron levels caused increased iron levels in the RPE, and, to a lesser extent, NR (because only *Tfrc* mRNA and

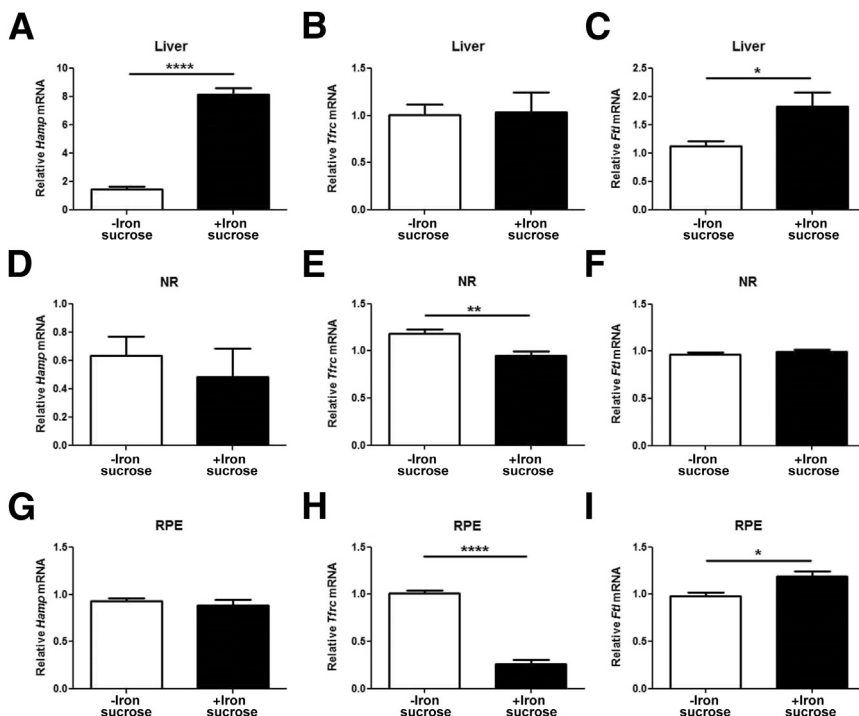


Figure 3 Quantitative PCR results in retina and RPE of i.v. iron sucrose–injected C57Bl/6J mice. Relative mRNA levels of *Hamp*, *Tfrc*, and L ferritin (*Ftl*) in the liver (A–C), NR (D–F), and RPE (G–I) of mice with or without iron sucrose injection. *Hamp* (A) and *Ftl* (C) mRNA levels in liver were significantly higher in mice with iron sucrose injection compared with controls. *B*: *Tfrc* mRNA levels in liver of mice with or without iron sucrose injection were not different. *Hamp* (D) and *Ftl* (F) mRNA levels in NR of mice with or without iron sucrose injection were not different. *E*: *Tfrc* mRNA levels were significantly lower in mice with iron sucrose injection compared with controls. *G*: *Hamp* mRNA levels in RPE of mice with or without iron sucrose injection were not different. *H*: *Tfrc* mRNA levels were significantly lower in the RPE of iron sucrose–injected mice compared with mice without iron sucrose injection. *I*: *Ftl* mRNA levels were significantly higher in the RPE of mice with iron sucrose injection compared with controls. Values shown are means \pm SEM of $\Delta\Delta C_T$. $N = 3$ biological and technical replicates for all real-time quantitative PCR experiments. * $P < 0.05$, ** $P < 0.01$, and **** $P < 0.0001$.

not the less sensitive measure L ferritin mRNA changed in the NR). Therefore, Hamp produced locally in the retina is insufficient to prevent retinal iron uptake in the context of increased blood iron levels. Although elevated iron levels in the liver are a strong stimulus for Hamp expression, after iron sucrose injection, Hamp mRNA levels in the NR were unaltered; the acute systemic iron challenge did not cause retinal Hamp up-regulation.

After i.v. iron injection, the oxidative stress markers MDA and HNE increase in the photoreceptor inner segments. The RPE accumulates more iron than the NR, but oxidative stress markers were not elevated in the RPE. It is likely that the RPE has a more robust antioxidant defense system than the photoreceptors.

These studies emphasize the importance of blood iron levels on retinal iron levels; elevated blood iron levels may cause increased retinal iron-induced oxidative stress levels. Elevated systemic iron levels, whether caused by genetics or diet, may increase the risk of age-related retinal disease, including age-related macular degeneration. In support of this possibility, people eating diets high in red meat, which causes high levels of iron absorption by the gut, have an increased risk of age-related macular degeneration.^{2,3}

Acknowledgment

Rabbit anti-L ferritin (E17) antibody was a gift from Dr. Paolo Arosio (University of Brescia, Brescia, Italy).

References

- Gnana-Prakasam JP, Martin PM, Smith SB, Ganapathy V: Expression and function of iron-regulatory proteins in retina. *IUBMB Life* 2010, 62:363–370
- Song D, Dunaief JL: Retinal iron homeostasis in health and disease. *Front Aging Neurosci* 2013, 5:24
- Hadziahmetovic M, Dentchev T, Song Y, Haddad N, He X, Hahn P, Pratico D, Wen R, Harris ZL, Lambris JD, Beard J, Dunaief JL: Ceruloplasmin/hephaestin knockout mice model morphologic and molecular features of AMD. *Invest Ophthalmol Vis Sci* 2008, 49: 2728–2736
- Hahn P, Qian Y, Dentchev T, Chen L, Beard J, Harris ZL, Dunaief JL: Disruption of ceruloplasmin and hephaestin in mice causes retinal iron overload and retinal degeneration with features of age-related macular degeneration. *Proc Natl Acad Sci U S A* 2004, 101:13850–13855
- Hadziahmetovic M, Song Y, Ponnuru P, Iacovelli J, Hunter A, Haddad N, Beard J, Connor JR, Vaulont S, Dunaief JL: Age-dependent retinal iron accumulation and degeneration in hepcidin knockout mice. *Invest Ophthalmol Vis Sci* 2011, 52:109–118
- Meynard D, Kautz L, Darnaud V, Canonne-Hergaux F, Coppin H, Roth M-P: Lack of the bone morphogenetic protein BMP6 induces massive iron overload. *Nat Genet* 2009, 41:478–481
- Hadziahmetovic M, Song Y, Wolkow N, Iacovelli J, Kautz L, Roth M-P, Dunaief JL: Bmp6 regulates retinal iron homeostasis and has altered expression in age-related macular degeneration. *Am J Pathol* 2011, 179:335–348
- Soe-Lin S, Apte SS, Andriopoulos B, Andrews MC, Schranzhofer M, Kahawita T, Garcia-Santos D, Ponka P: Nramp1 promotes efficient macrophage recycling of iron following erythrophagocytosis in vivo. *Proc Natl Acad Sci U S A* 2009, 106:5960–5965
- Gunshin H, Mackenzie B, Berger UV, Gunshin Y, Romero MF, Boron WF, Nussberger S, Gollan JL, Hediger MA: Cloning and characterization of a mammalian proton-coupled metal-ion transporter. *Nature* 1997, 388:482–488
- Donovan A, Brownlie A, Zhou Y, Shepard J, Pratt SJ, Moynihan J, Paw BH, Drejer A, Barut B, Zapata A, Law TC, Brugnara C, Lux SE, Pinkus GS, Pinkus JL, Kingsley PD, Palis J, Fleming MD, Andrews NC, Zon LI: Positional cloning of zebrafish ferroportin1 identifies a conserved vertebrate iron exporter. *Nature* 2000, 403:776–781
- Nemeth E, Tuttle MS, Powelson J, Vaughn MB, Donovan A, Ward DM, Ganz T, Kaplan J: Hepcidin regulates cellular iron efflux by binding to ferroportin and inducing its internalization. *Science* 2004, 306:2090–2093
- Ramos E, Kautz L, Rodriguez R, Hansen M, Gabayan V, Ginzburg Y, Roth M-P, Nemeth E, Ganz T: Evidence for distinct pathways of hepcidin regulation by acute and chronic iron loading in mice. *Hepatology* 2011, 53:1333–1341
- Pak M, Lopez MA, Gabayan V, Ganz T, Rivera S: Suppression of hepcidin during anemia requires erythropoietic activity. *Blood* 2006, 108:3730–3735
- Liu X-B, Nguyen N-BH, Marquess KD, Yang F, Haile DJ: Regulation of hepcidin and ferroportin expression by lipopolysaccharide in splenic macrophages. *Blood Cells Mol Dis* 2005, 35:47–56
- Gnana-Prakasam JP, Martin PM, Mysona BA, Roon P, Smith SB, Ganapathy V: Hepcidin expression in mouse retina and its regulation via lipopolysaccharide/Toll-like receptor-4 pathway independent of Hfe. *Biochem J* 2008, 411:79–88
- Hahn P, Dentchev T, Qian Y, Rouault T, Harris ZL, Dunaief JL: Immunolocalization and regulation of iron handling proteins ferritin and ferroportin in the retina. *Mol Vis* 2004, 10:598–607
- Solloway MJ, Dudley AT, Bikoff EK, Lyons KM, Hogan BLM, Robertson EJ: Mice lacking Bmp6 function. *Dev Genet* 1998, 22:321–339
- Dunaief JL, Dentchev T, Ying G-S, Milam AH: The role of apoptosis in age-related macular degeneration. *Arch Ophthalmol* 2002, 120: 1435–1442
- Xin-Zhao Wang C, Zhang K, Aredo B, Lu H: Ufret-Vincenty RL: novel method for the rapid isolation of RPE cells specifically for RNA extraction and analysis. *Exp Eye Res* 2012, 102:1–9
- Song D, Song Y, Hadziahmetovic M, Zhong Y, Dunaief JL: Systemic administration of the iron chelator deferiprone protects against light-induced photoreceptor degeneration in the mouse retina. *Free Radic Biol Med* 2012, 53:64–71
- Rouault TA: The role of iron regulatory proteins in mammalian iron homeostasis and disease. *Nat Chem Biol* 2006, 2:406–414
- Muckenthaler MU, Galy B, Hentze MW: Systemic iron homeostasis and the iron-responsive element/iron-regulatory protein (IRE/IRP) regulatory network. *Annu Rev Nutr* 2008, 28:197–213
- Chong EW-T, Simpson JA, Robman LD, Hodge AM, Aung KZ, English DR, Giles GG, Guymer RH: Red meat and chicken consumption and its association with age-related macular degeneration. *Am J Epidemiol* 2009, 169:867–876